



**HAL**  
open science

## Electron collisions with dimethylamine and trimethylamine molecules and molecular ions

Suliman M. Alshammari, Jean-Luc Le Garrec, James Brian Alexander Mitchell

► **To cite this version:**

Suliman M. Alshammari, Jean-Luc Le Garrec, James Brian Alexander Mitchell. Electron collisions with dimethylamine and trimethylamine molecules and molecular ions. *International Journal of Mass Spectrometry*, 2022, 474, pp.116802. 10.1016/j.ijms.2022.116802 . hal-03596264

**HAL Id: hal-03596264**

**<https://hal.science/hal-03596264>**

Submitted on 1 Apr 2022

**HAL** is a multi-disciplinary open access archive for the deposit and dissemination of scientific research documents, whether they are published or not. The documents may come from teaching and research institutions in France or abroad, or from public or private research centers.

L'archive ouverte pluridisciplinaire **HAL**, est destinée au dépôt et à la diffusion de documents scientifiques de niveau recherche, publiés ou non, émanant des établissements d'enseignement et de recherche français ou étrangers, des laboratoires publics ou privés.



Distributed under a Creative Commons Attribution - NonCommercial - NoDerivatives 4.0 International License

# Electron Collisions with Dimethylamine and Trimethylamine Molecules and Molecular Ions

*Suliman M. Alshammari*<sup>\* 1</sup>, *Jean-Luc Le Garrec*<sup>2, 3</sup> and *J. Brian A. Mitchell*<sup>4</sup>

<sup>1</sup>King Abdulaziz City for Science and Technology, P.O. Box 6086, Riyadh, 11442, Saudi Arabia

<sup>2</sup>Université de Rennes, CNRS, IPR (Institut de Physique de Rennes) UMR 6251, F-35000, France

<sup>3</sup>École des applications militaires de l'énergie atomique (EAMEA), Cherbourg, 50115, France

<sup>4</sup>Merl-Consulting SAS, Rennes, France 35000

**ABSTRACT:** Experiments are described in which the dissociative recombination of trimethylamine and dimethylamine ions and related product ions, was studied using a Flowing Afterglow Langmuir Probe- Mass Spectrometer (FALP-MS) apparatus. The technique used in this experiment is based on the measurement of the decay of the electron density as an afterglow plasma flows along a drift tube. The results obtained for the DR for dimethylamine and trimethylamine ions were measured using three different methods. The results for trimethylamine ions are in reasonable accord with those for other polyatomic ions while for dimethylamine ions, are unreasonably high and this was explained by the competition from electron capture by neutral dimethylamine molecules.

## *Keywords:*

Ion-Molecule reactions

Flowing Afterglow Langmuir Probe- Mass Spectrometer (FALP-MS)

Dissociative Recombination of ions with electrons (DR)

Dissociative Electron Attachment with neutral molecules (DEA)

Cluster ions

## 1. INTRODUCTION

Cloud formation is an important factor in climate science since they change the local albedo of the earth and of course are responsible for rainfall and other precipitations. The mechanisms behind the nucleation phenomena leading to cloud formation is an active subject therefore, in aerosol science. It has long been recognized, for example, that sulfuric acid ( $\text{H}_2\text{SO}_4$ ) in the upper atmosphere originating from industrial pollution volcanic activity, plays an important role in the initial nucleation process<sup>1</sup>. This has been demonstrated by both theoretical and experimental studies and the role of negative ions, generated by sunlight driven ionization processes, has been shown to act through the generation of acid/water cluster ions that acts as seeds for the generation of cloud condensation nuclei (CCN) the precursors of droplet formation.

---

\*Corresponding author email's: sshamari@kacst.edu.sa

Ammonia (generated from agricultural sources amongst others) has also been identified as a partner in this process, enhancing the nucleation rate<sup>2,3,4</sup>. In a series of experiments however, performed at the CERN laboratory in Geneva, where a beam of high energy particles is made to enter a large cloud chamber equipped with sophisticated chemical analysis equipment (mass spectrometers), it was found that the presence of dimethylamine<sup>5,6,7</sup> displayed a particularly strong catalytic activity, enhancing the nucleation rate by four orders of magnitude. Dimethylamine and trimethylamine are molecules emitted naturally in agriculture and also from decaying fish products. They can also be produced in the atmosphere through light induced chemical reactions involving ammonia. Because of this interest in dimethylamine (DMA) and trimethylamine (TMA), we decided to study the dissociative recombination of dimethylamine and trimethylamine ions using the Flowing Afterglow Langmuir Probe-Mass Spectrometer apparatus in the University of Rennes I since the rate coefficients for these ions have not been examined previously.

## 2. EXPERIMENT

The experimental apparatus has been described in detail before<sup>8</sup> and only a brief description is given here. The technique is an extension of the conventional FALP technique (Figure 1) that includes a moveable mass spectrometer which is used to identify ions present in the measurement region of the afterglow and to measure the number density of these ions as a function of distance along the flow. Electron concentration along the flow is measured using a Langmuir probe attached to the nose of the mass spectrometer.

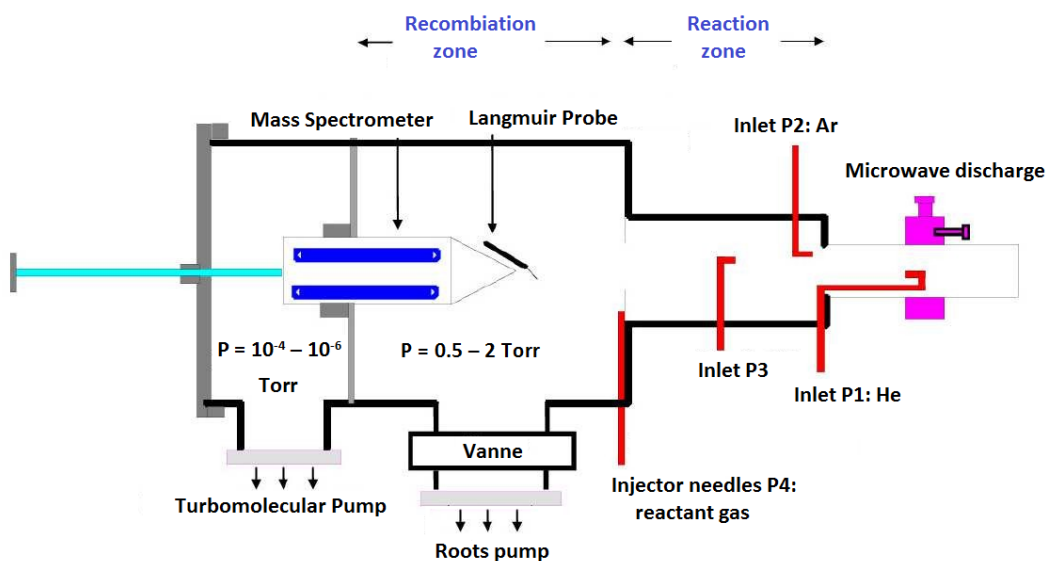


Fig. 1: Sketch of FALP-MS apparatus at University of Rennes<sup>8</sup>

In this experiment, helium gas was passed through a Zeolyte trap cooled to liquid nitrogen temperature to remove all impurities (water) and then introduced (inlet P1) at a rate of 24 sl min<sup>-1</sup>

<sup>1</sup>, into a 4.2 cm diameter glass tube surrounded by a microwave cavity operating at 2.45 GHz. The helium was then ionized by the microwave discharge. The helium gas flowed out of this tube and into an 8.5 cm diameter, 100 cm long, stainless steel chamber, the flow being established by means of a 4000 m<sup>3</sup>/h Roots pump. Typical operating pressures in the flow were from 0.50 to 0.60 Torr (corresponding to a helium density of 1.6 x 10<sup>16</sup> cm<sup>-3</sup> and 1.9 x 10<sup>16</sup> cm<sup>-3</sup> respectively) and that means that ions underwent many collisions with the buffer gas during their passage through the apparatus. The upstream region of the afterglow contained He<sup>+</sup>, He<sub>2</sub><sup>+</sup>, neutral metastable atoms He<sup>m</sup> and electrons.

Due to the helium buffer, the hot electrons in the plasma were cooled within a few μs by collisions and the condition where  $T_{gas} = T_{ion} = T_e$  was obtained. Argon gas was introduced at a second entry port (inlet P2), downstream, at a rate of 1 sl min<sup>-1</sup> in order to produce an Ar<sup>+</sup> dominated plasma via the reactions:

**Table 1:** Main reactions occur in conversion of the helium plasma to Ar<sup>+</sup> dominated plasma.

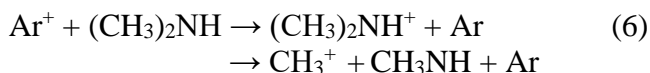
No	Reaction	Rate Coefficient (cm <sup>3</sup> s <sup>-1</sup> )	References
<b>He</b>			
1	He <sup>+</sup> + He + He → He <sub>2</sub> <sup>+</sup> + He	1 x 10 <sup>-31</sup>	[9]
2	He <sup>m</sup> + He <sup>m</sup> → He <sup>+</sup> + He + e <sup>-</sup>	5 x 10 <sup>-9</sup>	[10]
	→ He <sub>2</sub> <sup>+</sup> + e <sup>-</sup>	5 x 10 <sup>-9</sup>	[11]
<b>Ar</b>			
3	He <sup>m</sup> + Ar → He + Ar <sup>+</sup> + e	7 x 10 <sup>-11</sup>	[9]
4	He <sup>+</sup> + Ar → Ar <sup>+</sup> + He	1 x 10 <sup>-13</sup>	[12]
5	He <sub>2</sub> <sup>+</sup> + Ar → He + He + Ar <sup>+</sup>	2 x 10 <sup>-10</sup>	[9]

the argon atom density in the plasma being 0.85 x 10<sup>14</sup> cm<sup>-3</sup> for the measurements performed at 0.60 Torr and 0.7 x 10<sup>14</sup> cm<sup>-3</sup> for those performed at 0.5 Torr.

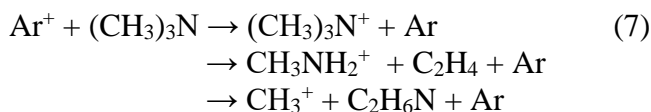
The absence of He<sub>2</sub><sup>+</sup> in the mass spectrum (in the measurement area, about 1 cm after the argon injection) verified that reaction (3) had gone to completion, prior to arriving at the measurement region. Given that He<sub>2</sub><sup>+</sup> is rapidly formed by reaction of He<sup>m</sup> with Ar (reaction 2) this is a good indication that the metastables had also been removed.

Thus, the helium plasma was converted into an argon plasma. The flow then entered a stainless-steel tube at the exit of which an eight-needle entry port (used to avoid aerodynamic perturbation) allowed us to add reactant gases in order to form the molecular ion under study. The identity of the ions formed was measured using the movable mass spectrometer and the electron number density was measured using a Langmuir Probe method. From these measurements, it is possible to determine the rate coefficients for reactions occurring in the flow and these shall be described in the next section.

The experimental conditions during the experiment were, pressure between 0.50 and 0.60 Torr, room temperature 300 K, electron density ( $1.5 \times 10^9 \text{ cm}^{-3} < n_e < 7.6 \times 10^9 \text{ cm}^{-3}$ ) and plasma velocity  $(1.85 \pm 0.15) \times 10^4 \text{ cm/s}$  (the central flow velocity of the plasma was determined by modulating the discharge and by measuring the time of flight of the resulting disturbance at the Langmuir probe, located on the central axis). Neutral DMA or TMA vapor phase molecules were injected downstream into the plasma without disturbing the aerodynamics of the flow and reacted with the primary ions ( $\text{Ar}^+$ ) present in the plasma leading to the formation of secondary ions via charge transfer processes<sup>9</sup> as seen in reactions (6 and 7).



and



### 3. DATA ANALYSIS

The actual measurement of the recombination coefficient in this apparatus can be performed in one of two ways<sup>13</sup>. For a pure plasma, containing a single ion that does not react with the neutral gas and in which the electron decay is dominated by recombination only, the decay of the electron density  $n_e$  with time,  $t$ , can be written as

$$\frac{dn_e}{dt} = -\alpha n_e^2 \quad (\text{I})$$

where  $\alpha$  is the recombination rate coefficient. Equation I is derived, assuming that the electron density is equal to the ion density (i.e., the plasma is neutral and does not contain negative ions) and that only a single ion is present. In a flowing afterglow, it is easy to measure the electron density at several places downstream of a given origin, using for example, a movable Langmuir probe. One can rewrite Eq. (I) in terms of the downstream distance,  $z$  and the plasma velocity,  $v$ , thus

$$v \frac{dn_e}{dz} = -\alpha n_e^2 \quad (\text{II})$$

Integrating Eq. (II) from some arbitrary origin  $z = z_0$  to some downstream position  $z$ , yields the following expression for  $n_e$ :

$$\left(\frac{1}{n_e}\right)_z = \left(\frac{1}{n_e}\right)_{z_0} + \frac{\alpha}{v} (z - z_0) \quad (\text{III})$$

Thus, the plot of  $1/n_e$  vs  $z$ , allows us to determine the recombination rate coefficient  $\alpha$  if the plasma velocity  $v$  is known.

In  $\text{DMA}^+$  and  $\text{TMA}^+$  plasma case, several ions were found to be present in the plasma where the secondary ions reacted with other neutral DMA or TMA molecules to form other ion fragments

such as clusters ions. The set of formation reactions for these ions is summarized in Table 2. Therefore, an alternative (and less restrictive) method used for determining the recombination rate from an afterglow measurement was as follows. One can write down the equation for the change in the density  $[AB^+]$  of the ions under study as a function of time,  $t$ , and therefore of distance,  $z$ , along the flow tube, thus

$$\frac{d[AB^+]}{dt} = v \frac{d[AB^+]}{dz} = -\alpha[AB^+]n_e - k[AB^+][X] - \frac{D_A}{\lambda^2} [AB^+], \quad (\text{IV})$$

where  $v$  is the plasma velocity, measured at the centerline of the flow,  $[X]$  the density of a reagent, such as an impurity with which the ion can undergo an ion–molecule reaction,  $n_e$  is the electron density,  $D_A$  is the coefficient of ambipolar diffusion and  $\lambda$  is the characteristic diffusion length. By integrating Eq. (IV) from some initial starting point,  $z_0$  to some position,  $z$ , one obtains the following solution:

$$v \ln \frac{[AB^+]_z}{[AB^+]_{z_0}} = -\alpha \int_{z_0}^z n_e dz - \left\{ k[X] + \frac{D_A}{\lambda^2} \right\} (z - z_0), \quad (\text{V})$$

where  $[AB^+]_z$  and  $[AB^+]_{z_0}$  are the ion number densities at position  $z$  and  $z_0$ , respectively.

It can be seen from this equation that if the ion–molecule reaction and diffusion losses are small compared to those due to recombination, the change in the number density of  $[AB^+]$  with distance is proportional to the integral of the electron density over  $z$ , from the starting point  $z_0$  to the point where the measurement is made. The constant of proportionality is  $\alpha/v$  where  $v$  is the velocity of the plasma. The crucial thing to notice about this method is that since the effects of ion–molecule reactions due to interaction with impurity species (or with one of the secondary plasma components), are independent of the electron density, they should not interfere with the determination of  $\alpha$ , provided one sees a decrease in the ion density as a function of distance along the flow. Even if diffusion losses are not small, as long as Eq. (V) is a good description of the ion decay process, the term due to diffusion remains constant and thus does not interfere with the determination of  $\alpha$ .

In this case, it is still possible to use Eq. (V) to determine  $\alpha$ , by measuring the ratio on the Left-Hand Side (LHS) but at a fixed value of  $z$  for different electron densities. Indeed, ion molecule reactions do not depend on the electron density but only on the density of the reactant gas and time, i.e. the position  $z$  in the reaction zone. Variation of the electron density in the flow can be achieved, in practice, by varying the position of the microwave cavity with respect to the helium inlet port (P1). In this method, the second term on the RHS is now constant (being independent of electron density) and only reactions involving electrons are taken into consideration. Therefore, assuming that electron attachment does not occur in these chemical reaction networks, only dissociative electron recombination plays a role in the evolution of both the ions and electron density.

This analysis is well suited to the study of ions which are not terminal and that are being produced and destroyed along the flow. Fixing a  $z$  position and varying the electron density allow the dissociative recombination rate coefficient to be determined, electron density being the only variable parameter. In fact, the rate coefficient for recombination was determined in most of the experiments, described in this report by measuring  $[AB^+]$  at a fixed  $z$  position for several different

electron densities as well as at variable z positions for a given electron density, for a known plasma velocity.

**Table 2:** Main reactions taking place in the formation of DMA<sup>+</sup> and TMA<sup>+</sup> ions.

No	Reaction	Rate Coefficient (cm <sup>3</sup> s <sup>-1</sup> )	Ref
<b>DMA<sup>+</sup> formation</b>			
8	$\text{CH}_3^+ + (\text{CH}_3)_2\text{NH} \rightarrow (\text{CH}_3)_2\text{NH}_2^+ + \text{CH}_2$	$2.10 \times 10^{-9}$	[14]
9	$(\text{CH}_3)_2\text{NH}^+ + (\text{CH}_3)_2\text{NH} + \text{He} \rightarrow ((\text{CH}_3)_2\text{NH})_2^+ + \text{He}$	-	-
<b>TMA<sup>+</sup> formation</b>			
10	$\text{CH}_3^+ + (\text{CH}_3)_3\text{N} \rightarrow (\text{CH}_3)_3\text{NH}^+ + \text{CH}_2$	$6.30 \times 10^{-10}$	[15]
11	$\text{CH}_3\text{NH}_2^+ + (\text{CH}_3)_3\text{N} \rightarrow (\text{CH}_3)_3\text{N}^+ + \text{CH}_3\text{NH}_2$ $\rightarrow (\text{CH}_3)_3\text{NH}^+ + \text{CH}_2\text{NH}_2$	$1.60 \times 10^{-9}$	[16]
12	$(\text{CH}_3)_3\text{N}^+ + (\text{CH}_3)_3\text{N} \rightarrow (\text{CH}_3)_3\text{NH}^+ + (\text{CH}_3)_2\text{NCH}_2$	$1.50 \times 10^{-9}$	[16]
13	$(\text{CH}_3)_3\text{N}^+ + (\text{CH}_3)_3\text{N} \rightarrow \text{products}$	$8.20 \times 10^{-10}$	[17]
14	$(\text{CH}_3)_3\text{NH}^+ + (\text{CH}_3)_3\text{N} \rightarrow ((\text{CH}_3)_3\text{N})_2 \cdot \text{H}^+$	-	[18]

## 4. RESULTS AND DISCUSSION

### 4.1 Measurements of the DR Rate Coefficient for TMA Molecular Ions

The reactant gas was mixed with helium in the required ratio (TMA gas diluted with He gas at a ratio of about 1:50) before injection into the flow tube with flow rates such as to obtain densities of TMA molecules in the range  $\sim 1.4 - 4 \times 10^{12} \text{ cm}^{-3}$ .

In our plasma, and for a TMA gas density of  $1.4 \times 10^{12} \text{ cm}^{-3}$ , it was found that ion-molecule reactions of the Ar<sup>+</sup> dominated plasma with neutral TMA molecules, generated (CH<sub>3</sub>)<sub>3</sub>N<sup>+</sup> (m/q=59), protonated trimethylamine (CH<sub>3</sub>)<sub>3</sub>NH<sup>+</sup> (m/q =60) and other fragments ions such as CH<sub>3</sub><sup>+</sup> (m/q=15), CH<sub>3</sub>NH<sup>+</sup> (m/q=30), methylamine CH<sub>3</sub>NH<sub>2</sub><sup>+</sup> (m/q=31) and (CH<sub>2</sub>)<sub>3</sub>NH<sup>+</sup> (m/q =57). as shown in Figure 2.

The formation of some of the major ion products of the reaction of Ar<sup>+</sup> with (CH<sub>3</sub>)<sub>3</sub>N via charge transfer reactions can be explained by reaction (7). Ion products such as CH<sub>3</sub><sup>+</sup> and methylamine CH<sub>3</sub>NH<sub>2</sub><sup>+</sup> reacting with neutral TMA molecules, lead to the production of more TMA molecular ions and protonated TMA ions as can be seen in reaction (10 and 11). The mass spectrum thus obtained is shown in Figure 2.

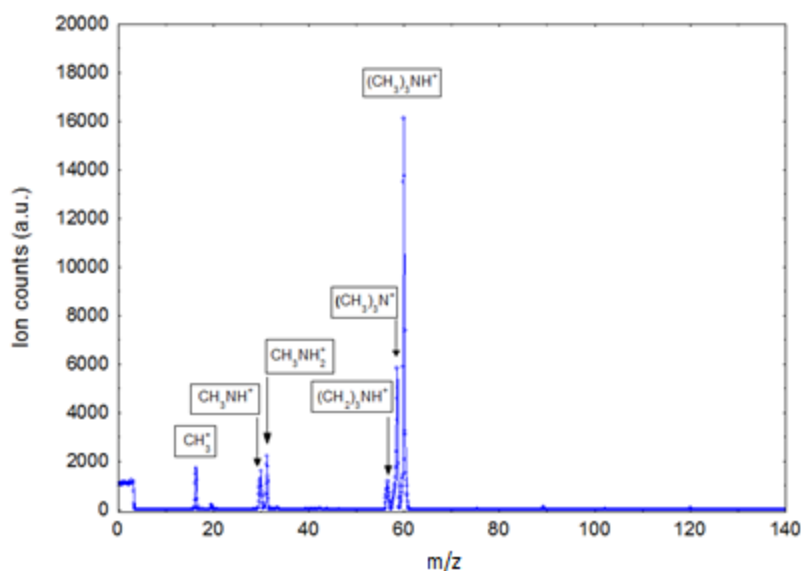


**Fig. 2:** Mass spectrum in the reaction chamber for a trimethylamine density of  $1.4 \times 10^{12} \text{ cm}^{-3}$  taken at 30 mm downstream from the injection port of the TMA/He mixture into an  $\text{Ar}^+$  dominated plasma.

In order to remove all the precursor ions in the reaction zone, the number density of TMA molecules was increased to  $4.0 \times 10^{12} \text{ cm}^{-3}$  and, the ion peaks then found in the mass spectrum measured at  $z_0 = 30 \text{ mm}$  are attributed to  $\text{TMA}^+$  ( $m/q = 59$ ) ion, protonated TMA ( $m/q = 60$ ) ion and to the cluster ions  $((\text{CH}_3)_3\text{N})_2^+$  ( $m/q = 118$ ),  $((\text{CH}_3)_3\text{N})_2\text{H}^+$  ( $m/q = 119$ ). We found that the signal peaks of  $\text{TMA}^+$  and protonated ions were reduced when moving the mass spectrometer further downstream from the injection port of TMA mixture and this loss, due to the reaction with neutral TMA molecules and electrons and indeed further clustering, can be seen in Figure 3.

It should be noted that in this experiment, there are many ions present in the measurement region and that these ions react with other molecules to form cluster ions.

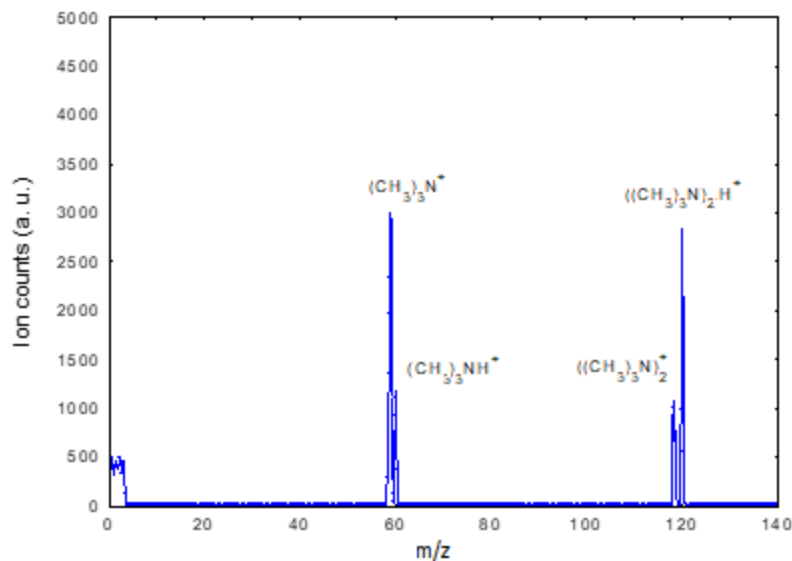


**Fig. 3:** Mass spectrum in the reaction chamber for a trimethylamine density of  $4.0 \times 10^{12} \text{ cm}^{-3}$  taken at 30 mm downstream from the injection port of the TMA/He mixture into an  $\text{Ar}^+$  dominated plasma.

Given that several ions were seen to be present in the mass spectra, the measurement protocol was applied for multiple ions present in the plasma as described in equation V. In the FALP-MS at room temperature and at a relatively high pressure of He and TMA, the formation of cluster ions via a three-body association reactions and their destruction by ion-molecule reactions with neutral TMA molecules and recombination with electrons can play an essential role. In such cases, we have to consider the reactions (10-14).

The balance equation for the studied ion (i.e.  $\text{TMA}^+$ ) can be written as:

$$\ln\left(\frac{[\text{TMA}^+]_z}{[\text{TMA}^+]_{z_0}}\right) = -\frac{\alpha}{v} \int_{z_0}^z n_e dz - \frac{1}{v} \left( k[\text{TMA}] + \frac{D_A}{\Lambda^2} \right) (z - z_0) \quad (\text{VI})$$

Values for the recombination rate coefficient were determined in several measurements where  $\ln\left(\frac{[\text{TMA}^+]_z}{[\text{TMA}^+]_{z_0}}\right)$  was plotted as a function of  $\int_{z_0}^z n_e dz$  measured for multiple  $z$  positions. Figure 4 shows an example such a plot<sup>1</sup>. Knowing the plasma velocity, the recombination rate coefficient  $\alpha$  is obtained from the slope of this plot.

<sup>1</sup> Similar plots were obtained  $\ln([\text{TMA.H}^+]_z/[\text{TMA.H}^+]_{z_0})$  versus  $\int n_e dz$ . In the following, only plots for the primary ions are presented, those for other ions studied being similar.

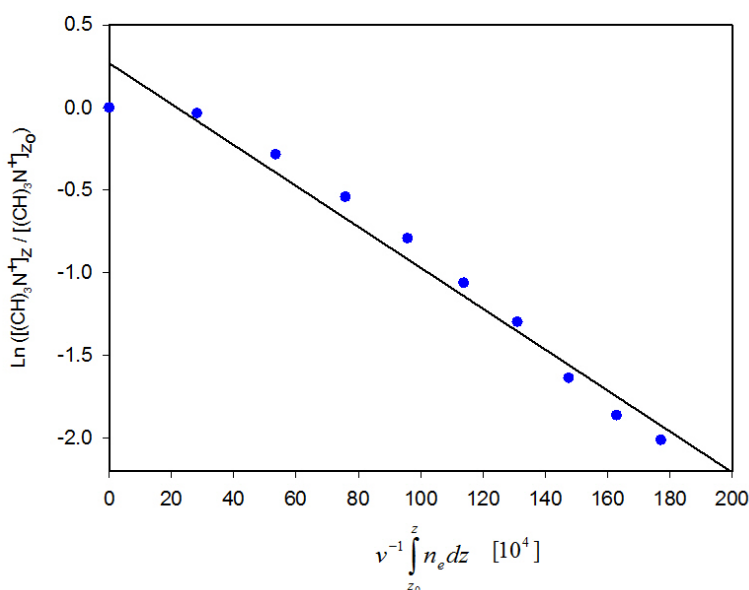


**Fig. 4:** Plot of the logarithm of  $[(CH_3)_3N^+]_z$  over  $[(CH_3)_3N^+]_{z_0}$  as a function of the electron density integral divided by the plasma velocity ( $v = 1.85 \cdot 10^4$  cm/s). The slope gives the rate coefficient for dissociative recombination of  $(CH_3)_3N^+$ .

These measurements however, do not take into account the influence of ion-molecule reactions (in this case clustering) which also lead to a change of  $[TMA^+]$  as a function of  $z$ . Hence the multiple ion/fixed  $z$  method was employed to yield the recombination rate coefficient. In this case the only variable is the electron number density which is independent of ion-molecule reactions and so the latter can be ignored. As described above, the upstream electron number density was varied while monitoring the ion number density of  $TMA^+$  or  $TMA.H^+$  at fixed  $z$ . The plots of  $\ln([TMA^+]_z / [TMA^+]_{z_0})$  and  $\ln([TMA.H^+]_z / [TMA.H^+]_{z_0})$  versus integrated electron density yield  $\alpha/v$  as the slope. The measurement was performed with several initial electron densities ( $4.5, 5.9$  and  $7.6 \times 10^9$  cm $^{-3}$ ) at fixed  $z$ , and the results obtained were found to yield linear plots as shown (for  $TMA^+$ ) in Figure 5.

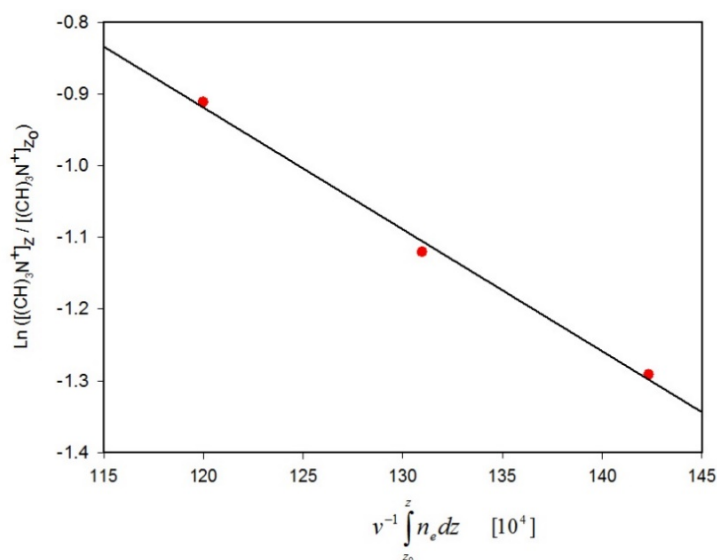


**Fig. 5:** The ratio of the density of  $[(\text{CH}_3)_3\text{N}^+]$  at a single value of  $z = 90$  mm downstream from the origin to the density at  $z_0$  vs the integral of the electron density from  $z_0$  to  $z$ , for three different initial electron densities, 4.5, 5.9 and  $7.6 \times 10^9 \text{ cm}^{-3}$ .

Within the accuracy of the FALP-MS measurements, the recombination rate coefficient for  $\text{TMA}^+$  ion and  $\text{TMA.H}^+$  were measured several times and the mean values are presented in Table 3. The values quoted include combined statistical and systematic uncertainties.

**Table 3:** Measured recombination rate coefficient for  $\text{TMA}^+$  and  $\text{TMA.H}^+$  ions at  $T = 300$  K. In this case, statistical errors of 30% are quoted.

Ion	Number of data points	Recombination rate coefficient [ $10^{-6} \text{ cm}^3 \text{ s}^{-1}$ ]	
		Multiple ions/z variable method	Multiple ions/fixe d z method
$(\text{CH}_3)_3\text{N}^+$	7	$1.3 \pm 0.4$	$1.6 \pm 0.5$
$(\text{CH}_3)_3\text{NH}^+$	7	$1.5 \pm 0.4$	$1.5 \pm 0.4$

The values of DR rates obtained by both methods were consistent for these two ions and so it would seem that the effects of diffusion or ion–molecule reactions do not have a major effect on the measurements in this case. Our measured rates coefficients for  $\text{TMA}^+$  and  $\text{TMA.H}^+$  are in reasonable accord with those for other polyatomic ions<sup>19</sup> (e.g.  $1.4 \times 10^{-6} \text{ cm}^3 \text{ s}^{-1}$  for  $\text{CH}_3\text{NH}_3^+$ ). Equation I, does not take into account, any electron loss effects due to electron attachment. To check if this was justified, the voltages on the mass spectrometer were inverted and a search was made for negative ions. No negative ions were found in the TMA plasma. Therefore, we can say that there was no electron attachment to the neutral TMA molecule found in our measurements and in fact this observation is borne out by measurements made by other workers<sup>20</sup>.

## 4.2 Measurements of DR Rate Coefficient for DMA Molecular Ions

It was found that dimethylamine vapor, when introduced at a density of  $1.7 \times 10^{12} \text{ cm}^{-3}$  via the eight-needle entry port into the sampling region of the apparatus, reacted with argon ions, producing several ions including  $\text{CH}_3^+$  ( $m/q = 15$ ) and  $(\text{CH}_3)_2\text{NH}^+$  ( $m/q = 45$ ) which went on to react with the parent dimethylamine vapor to produce species such as  $\text{CH}_3\text{NH}^+$  ( $m/q = 30$ ),  $(\text{CH}_3)_2\text{NH}_2^+$  ( $m/q = 46$ ) and dimer  $((\text{CH}_3)_2\text{NH})_2^+$  ion ( $m/q = 90$ ), and these could be described by reactions (7, 10 and 11), and the mass spectra for these ion masses shown in Figure 6.

It is seen that the parent molecule  $(\text{CH}_3)_2\text{NH}^+$  and the dimer  $((\text{CH}_3)_2\text{NH})_2^+$  ions are the majority ions and all other fragment ions are much less abundant. The main purpose for introducing the low density of DMA was to explore the formation of source ions (such as  $\text{CH}_3^+$ ) which react very fast to form the major product ions. Figure 6 is plotted for several different  $z$  positions and it is seen that the peaks with mass less than or equal to 40, disappear downstream, the  $\text{DMA}^+$  peak decreases regularly and the dimer ion peak increases. The trimer ions peak is also seen to grow.

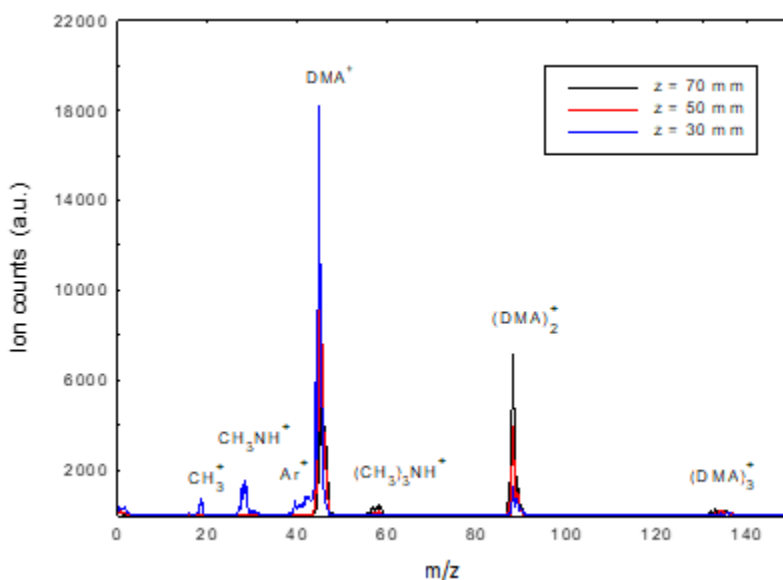


**Fig. 6:** Mass spectrum in the reaction chamber for a dimethylamine density of  $1.7 \times 10^{12} \text{ cm}^{-3}$  taken at different  $z$  positions downstream from the injection port of the DMA/He mixture into an  $\text{Ar}^+$  dominated plasma.

By increasing the density of dimethylamine to  $4.5 \times 10^{12} \text{ cm}^{-3}$ , a spectrum was found with,  $(\text{CH}_3)_2\text{NH}^+$ , ( $m/q = 45$ )  $(\text{CH}_3)_3\text{NH}^+$  ( $m/q = 60$ ) and the cluster ions  $((\text{CH}_3)_2\text{NH})_2^+$  ( $m/q = 90$ ),  $((\text{CH}_3)_2\text{NH})_3^+$  ( $m/q = 135$ ) and the source of most these ions disappeared as shown in Figure 7.

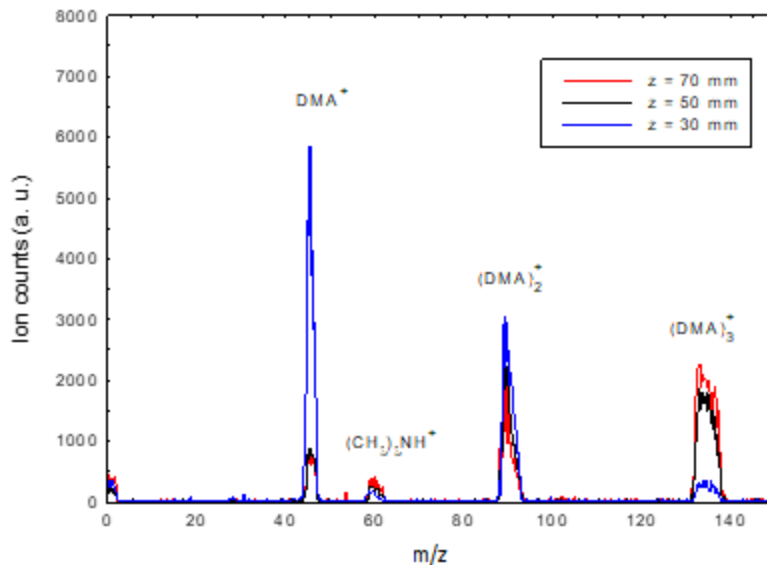


**Fig. 7:** Mass spectrum in the reaction chamber for a dimethylamine density of  $4.5 \times 10^{12} \text{ cm}^{-3}$  taken at different  $z$  positions downstream from the injection port of the DMA/He mixture into an  $\text{Ar}^+$  dominated plasma.

It can be seen that when the dimethylamine concentration was increased, the mass 45 amu and 90 amu peaks due to the  $\text{DMA}^+$  ion and the dimer  $(\text{DMA})_2^+$  were seen to decrease (the dimer peaks much less rapidly than the monomer peak) while the mass 135 amu due to the  $(\text{DMA})_3^+$  ion, was seen to increase. This is because the dimer  $(\text{DMA})_2^+$  ion is present in large abundance and reacted continually with neutral DMA molecules to form the  $(\text{DMA})_3^+$ .

The decrease of the  $(\text{DMA})_3^+$  ion signal could be seen at higher density of DMA and it also could possibly be undergoing further reactions with neutral DMA molecules to produce further clustering beyond our measurable mass range. The mass 60 amu due to  $(\text{CH}_3)_3\text{NH}^+$  increases slightly downstream.

The experiment was performed with a dimethylamine density of  $4.5 \times 10^{12} \text{ cm}^{-3}$  and at initial electron number density of  $1.5 \times 10^9 \text{ cm}^{-3}$ . Using the multiple ion/  $z$  variable method, from several measurements we found the average value for the apparent recombination rate coefficient for the  $(\text{CH}_3)_2\text{NH}^+$  ion was  $5 \times 10^{-5} \text{ cm}^3\text{s}^{-1}$ , for  $((\text{CH}_3)_2\text{NH})_2^+$ ,  $6.5 \times 10^{-5} \text{ cm}^3\text{s}^{-1}$  and for  $((\text{CH}_3)_2\text{NH})_3^+$   $5.4 \times 10^{-5} \text{ cm}^3\text{s}^{-1}$ . An example of these measurements is shown (for  $\text{DMA}^+$ ) in Figure 8.

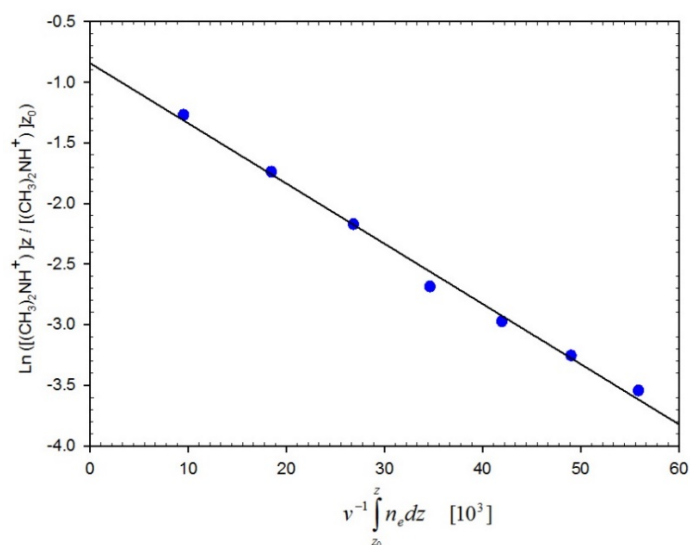


**Fig. 8:** Plot of the logarithm of  $[(\text{CH}_3)_2\text{NH}^+]$  at position  $z$  over  $[(\text{CH}_3)_2\text{NH}^+]$  at position  $z_0$  as a function of the electron density integral divided by the plasma velocity ( $v=1.85 \times 10^4$  cm/s). The slope gives the rate coefficient for dissociative recombination of  $(\text{CH}_3)_2\text{NH}^+$ .

In fact, these rates are considered to be unreasonably high as such values have never been seen for ground state monomer ions. Indeed, never even for highly clustered ions<sup>21</sup>. As a check, the multiple ions/ fixed  $z$  method was applied and the results for both methods (illustrated for  $\text{DMA}^+$  in Figure 9) are summarized in Table 4.

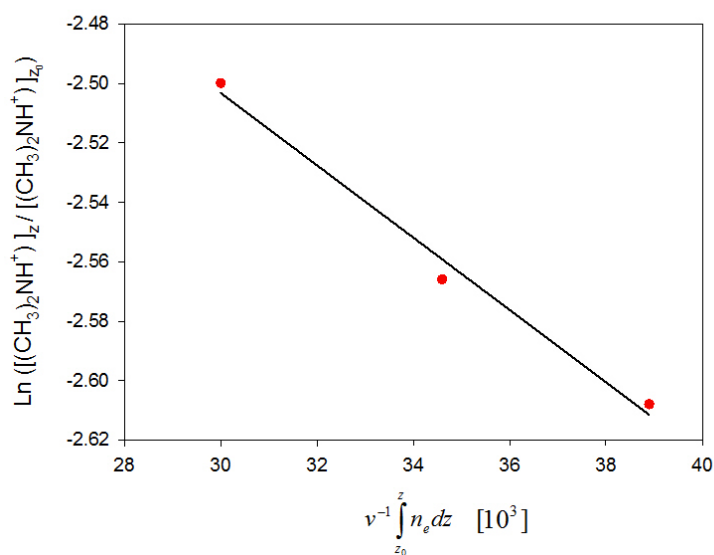


**Fig. 9:** The ratio of the density of  $[(\text{CH}_3)_2\text{NH}^+]$  at a single value of  $z = 70$  mm downstream from the origin to the density at  $z_0$  vs the integral of the electron density from  $z_0$  to  $z$ , for three different initial electrons densities.

**Table 4:** Measured values of apparent recombination rates determined using the methods of multiple ions present in the plasma. Fitting errors are quoted to allow a comparison to be made between the individual measurements. Note that these values are just given as apparent output from the method and should in no way be considered as real as the method has yielded values which are abnormally high.

Ion	Number of data points	Apparent recombination rate coefficient [ $10^{-5} \text{ cm}^3 \text{ s}^{-1}$ ]	
		Multiple ions/z variable method	Multiple ions/fixed z method
$(\text{CH}_3)_2\text{NH}^+$	10	$5.0 \pm 1.5$	$1.3 \pm 0.4$
$((\text{CH}_3)_2\text{NH})_2^+$	10	$6.5 \pm 2.0$	$2.8 \pm 0.8$
$((\text{CH}_3)_2\text{NH})_3^+$	10	$5.4 \pm 1.5$	$1.6 \pm 0.5$

It is seen that unlike the case for TMA ions, the values obtained are quite different, being between 2 and 4 times smaller. This still leaves unreasonably large apparent rate coefficients for the DMA monomer, dimer and trimer ions examined. For this reason, it was decided to check to see if there could be interference due to electron attachment which would compete with DR for electron removal and hence yield over-determined values.

The polarity of the quadrupole mass analyser was inverted (from negative to positive ion mode). In this case, it was found that a negative ion was present in the plasma, namely  $\text{HCNH}^-$  at  $m/q = 28$  amu as shown in Figure 10, indicating the presence of the electron attachment processes in the plasmas, forming negative ions. It was indeed observed that the negative ion counting rate increased regularly as the mass spectrometer was moved from the needle entry port position to the downstream part of the flow. Given this observation it was decided to examine the electron attachment process in more detail and to obtain its rate coefficient.

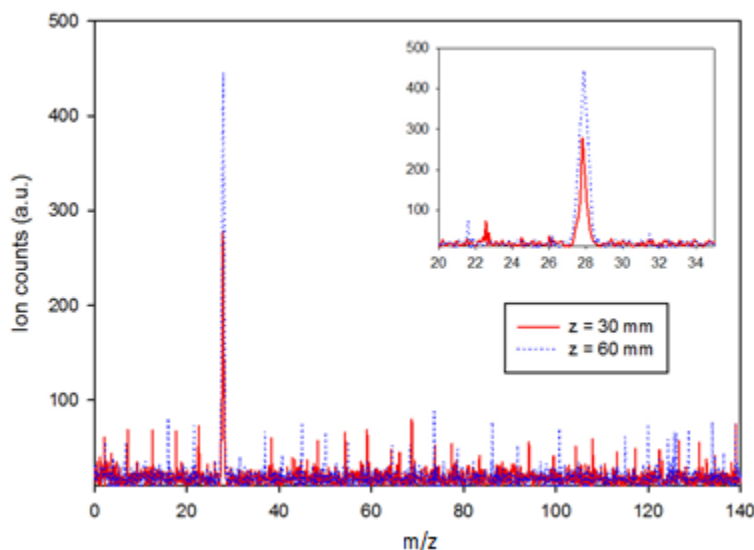


**Fig. 10:** Evolution of the  $\text{HCNH}^-$  ion at two different z position downstream from the injection port of DMA mixture with a neutral DMA density of  $4.5 \times 10^{12} \text{ cm}^{-3}$ .

### 4.3 Electron Attachment to Neutral DMA Molecule

Although our FALP-MS apparatus is essentially dedicated to studying the dissociative recombination process, it is also possible to measure the rate coefficient for electron attachment reactions. The coefficient rate  $\beta$  for electron attachment with neutral DMA molecule was obtained by introducing into the plasma flow (dominated by  $\text{Ar}^+$  ions), a mixture composed of dimethylamine  $(\text{CH}_3)_2\text{NH}$  and helium gas (the ratio of DMA/He mixture was about 1:50).

Since  $[\text{DMA}] \gg [\text{DMA}^+]$ , as a first crude approximation, one can ignore the influence of recombination in the plasma compared to that of electron attachment<sup>21,22</sup>, and in this case, the electron density,  $n_e$  would vary as a function of neutral DMA density  $[\text{DMA}]$ , as

$$\frac{dn_e}{dt} = v \frac{dn_e}{dz} \sim -\beta [\text{DMA}]n_e \quad (\text{VII})$$

where  $\beta$  is the attachment rate coefficient and it is assumed that diffusion is negligible. After integration, equation VII is reduced to:

$$\ln(n_e)_z = \ln(n_e)_{z_0} - \left( \frac{\beta [\text{DMA}] z}{v} \right), \quad (\text{VIII})$$

where  $z_0$  is the position where the first measurement is performed. The plot of  $\ln(n_e)_z$  versus  $z$  would therefore yield a straight line whose slope is  $-\beta [\text{DMA}]/v$ . Performing measurements of electron density decay for different DMA densities in the flow would give a series of lines with negative slopes. Figure 11 shows these series of lines at different DMA densities in the flow. The slopes of these lines yield the first order electron attachment rate coefficient  $k_{1st}$ .

$$k_{1st} = -\beta [\text{DMA}]/v \quad (\text{IX})$$

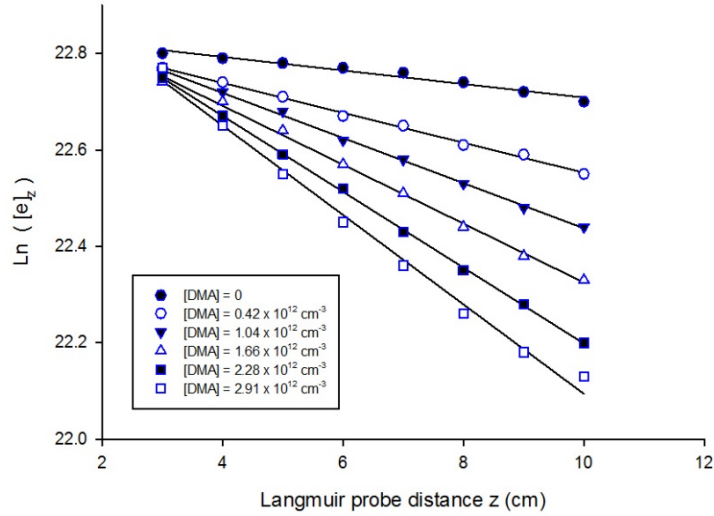


**Fig. 11:** Plots of the logarithm of different electron densities for different DMA concentrations as a function of different  $z$  positions along Langmuir probe distance.

By plotting these negative slopes which are obtained from equation IX as a function of neutral DMA density, we obtained a straight line as expected (see Figure 12) for which its slope is  $-\beta / v$ . Then, by multiplying it by the plasma velocity  $v$  (in our measurements,  $v = 1.85 \times 10^4$  cm/s), we get the electron attachment rate coefficient ( $\beta$ ). We performed two such measurements and the mean value of  $\beta$  was found to be  $(5.0 \pm 1.5) \times 10^{-10}$  cm<sup>3</sup> s<sup>-1</sup> taking into account an uncertainty of about 30%.

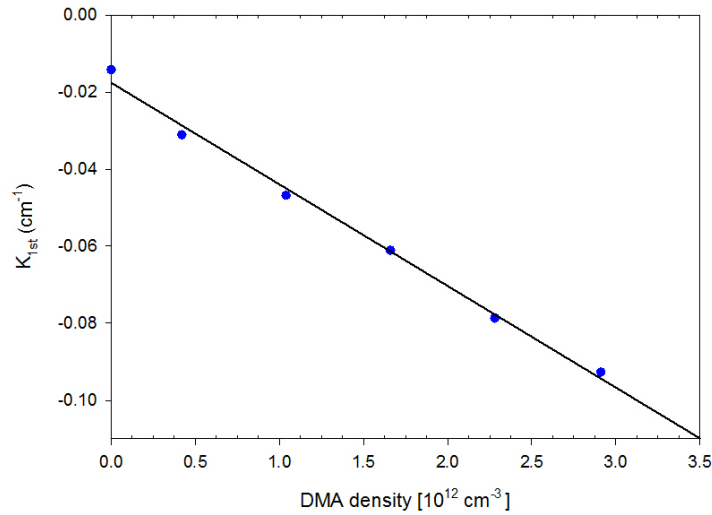


**Fig. 12:** Plot of the  $k_{1st} = -\beta [\text{DMA}] v$  as a function of the different DMA densities. The slope ( $\beta / v$ ) of this plot multiplied by plasma velocity ( $v = 1.85 \times 10^4$  cm/s) gives us the electron attachment rate. In this example ( $\beta = 4.8 \times 10^{-10}$  cm<sup>3</sup> s<sup>-1</sup>).

The value of  $\beta$  obtained with an initial electron density of  $7.5 \times 10^9 \text{ cm}^{-3}$  can be considered to be an upper limit of the electron attachment value. This is because we have neglected recombination which also reduces the measured electron density.

#### 4.4 Calculation of the Actual Recombination Rate for DMA Molecular Ions

In this section we shall examine the possibility of extracting the actual recombination coefficient for DMA ions assuming that it is not so large as to render the attachment rate determination uncertain. To perform this modelling we can consider the change of electron density with time ( $\frac{dn_e}{dt}$ ) as a function of both the recombination of electrons with the DMA ions and electron attachment with neutral DMA:

$$\frac{dn_e}{dt} = - [\sum_i \alpha_i M_i^+] n_e - \beta [M] n_e, \quad (\text{X})$$

where the  $[\sum_i M_i^+]$  is the sum of the ion densities in the plasma and  $[M]$  is the neutral density. We can take equation X and re-write it in the form:

$$- [\sum_i \alpha_i^{measured} M_i^+] n_e = - [\sum_i \alpha_i^{real} M_i^+] n_e - \beta^{measured} [M] n_e \quad (\text{XI})$$

We can insert the values from Table 3, for example  $\rightarrow \sum_i \alpha_i^{measured} \sim 5.7 \times 10^{-5} \text{ cm}^3 \text{ s}^{-1}$ ,  $\beta = 5 \times 10^{-10} \text{ cm}^3 \text{ s}^{-1}$  and  $[M] = 4.5 \times 10^{12} \text{ cm}^{-3}$ , and let us say that the actual rate coefficient for the recombination of  $\text{DMA}^+$  is  $1 \times 10^{-6} \text{ cm}^3 \text{ s}^{-1}$ , in line with that for  $\text{TMA}^+$  with those for the dimer and trimer ions being  $2 \times 10^{-6}$ . Thus:

$$-5.7 \times 10^{-5} [\sum_i M_i^+] = -5 \times 10^{-6} [\sum_i M_i^+] - 5 \times 10^{-10} \times 4.5 \times 10^{12},$$

which gives:

$$[\sum_i M_i^+] = 4.8 \times 10^7 \text{ cm}^{-3}$$

However, the typical initial electron density in these experiments was  $1.5 \times 10^9 \text{ cm}^{-3}$ , i.e. a factor of 30 greater. One possibility is that there are other heavier cluster ions which are beyond the mass range of our mass spectrometer but these would contribute to both sides of equation XI and so it is unlikely, though impossible to verify, that this would compensate for this discrepancy. Equations X and XI of course neglect the fact that when there is an attaching gas in the plasma, some of the negative charge resides with the negative ions formed, thus:

$$n_e + \sum_j [M_j^-] = \sum_i [M_i^+]$$

## 4.5 Negative ion products

As mentioned above, when searching for negative ions with DMA, only  $\text{HCNH}^-$  was found. In fact, the formation of  $\text{HCNH}^-$  is endothermic by about 4 eV. How then could such an endothermic channel appear? Firstly, it should be noticed that the observed signal for  $\text{HCNH}^-$  (Figure 10) is very much weaker than typical positive ion signals routinely measured in this apparatus (Figures 6,7). This suggests that this is very much a minority process. More important however, is the fact that the FALP-MS apparatus operates with a movable mass spectrometer which is used not only to identify the ions in the plasma but also as a means of determining rate coefficients. This mass spectrometer is illustrated schematically in Figure 13.

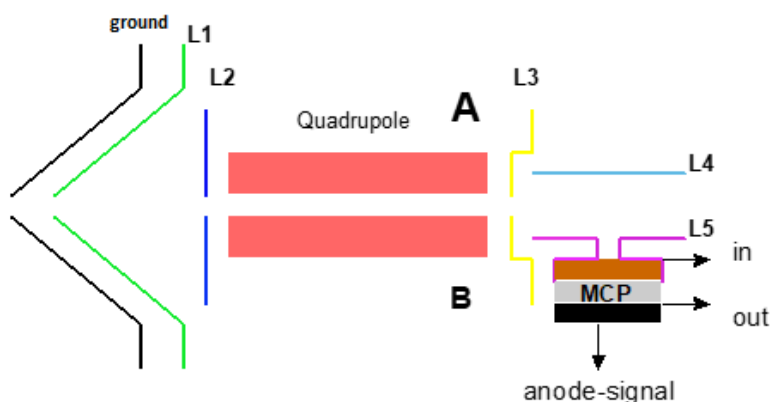


**Fig. 13:** Schematic of the lens structure of the quadrupole mass analyser in the FALP-MS apparatus.

The ions in the plasma enter the instrument, contained in a differentially pumped, movable vacuum chamber, via the grounded inlet cone. During operation, various voltages are applied to the electrodes L1-L5. In these experiments,  $\pm 2$  volts were applied to the electrode L1 in order to draw in the negative/positive ions and then  $\pm 50$  volts to the aperture L2 (and to L3) so that the ions would have sufficiently velocity to be analysed by the radiofrequency quadrupole analyser<sup>2</sup>. Hence ions entering the instrument are accelerated and if they collide with an aperture, and are thus dissociated by ion-surface collisions, it is possible that an endothermic channel can be accessed. Positive ions and cluster ions are robust structures and such a dissociation is less likely to occur than for negative ions where the binding energy of the attached electron is typically less than a few electron volts at most. In particular, negative clusters are expected to be fragile and we believe that this acceleration necessary for the operation of the mass spectrometer, is responsible for the disintegration of these clusters, entering the instrument, (by both surface and buffer gas collisions) so that we were not able to observed them. This is a known problem in mass spectrometer-based studies of cluster ions and particularly of negative cluster ions<sup>23</sup>. Hence, given

<sup>2</sup> (L4 is used to deflect ions exiting from the quadrupole analyser into the multi-channel plate detector (MCP) and a voltage of about  $\pm 2.5$  kV is applied to L5 to accelerate them so that they can be efficiently detected).

this addition of kinetic energy to the ions (and in particular for the case of negative ions), it is possible for the dissociation to an endothermic channel to be observed.

This suggests that the formation of  $\text{HCNH}^-$  is a rather rare reaction path and that other products are formed in the electron attachment, which are not seen. Although positive cluster ions are seen in the mass spectrum shown in Figure 7, negative cluster ions are not seen in the mass spectrum for negative ions shown in Figure 10. This could be because these ions would be destroyed by field induced electron detachment and collisions during the ion sampling process. Positive cluster ions are much more stable than negative cluster ions. A lightly bound electron could be stripped off during the ion sampling processes, and the resulting neutral cluster would dissociate. Thus we were able to see positive cluster ions though not negative ions. This is clearly a subject of speculation at this stage and will eventually be the subject of further study.

## 5. DISCUSSION AND CONCLUSION

In this study, we have measured the absolute rate coefficients for the dissociative recombination of trimethylamine and protonated trimethylamine cations with electrons. They are respectively,  $\alpha_1 = (1.3 \pm 0.4) \times 10^{-6} \text{ cm}^3\text{s}^{-1}$  and  $\alpha_2 = (1.5 \pm 0.5) \times 10^{-6} \text{ cm}^3\text{s}^{-1}$  taking into account the total measurement uncertainty of 30%. The measurements were performed using two techniques as discussed in the text (method B and C) and the obtained values for recombination rate were consistent for a given ion (see Table 2). A search was made for electron attachment to neutral TMA was made but no evidence for this was found indicating that this process is negligible in the Ar/TMA plasma chemistry.

On the other hand, the electron attachment to the neutral dimethylamine molecule was studied and we found that the parent molecule does undergo electron attachment, and this produces electron loss and so interferes with the recombination measurement. The measured rate for electron attachment was  $(5.0 \pm 1.5) \times 10^{-10} \text{ cm}^3 \text{ s}^{-1}$ . Rate coefficients for the dissociative recombination of dimethylamine and cluster ions with electrons were measured using methods B and C but the values obtained were anomalously high (several  $\times 10^{-5} \text{ cm}^3\text{s}^{-1}$ ) even for polyatomic ions and so we should ignore these. A possible explanation has been presented for this involving the mutual neutralisation of negative and positive cluster ions, the effect of which would not be eliminated by method C. Thus, although we have been able to measure the rate coefficient for electron attachment and we have not been able to give a rate coefficient for the DR of DMA ions.

What is clear from our measurements is that DMA is a molecule which clusters very easily, and in the upper atmosphere it can be ionized, for example by cosmic rays or other ionization processes or attach electrons to form negative ions which then form negative clusters though we have only been able to speculate on this. This fact is perhaps the reason that the influence of DMA in the upper atmosphere is to increase the rate of nucleation of water droplets and thus the formation of clouds<sup>3,5</sup>. This is a phenomenon which deserves further study of the underlying chemical processes and will be the subject of follow-on research to be conducted in the new accelerator laboratory in the KACST laboratory in Riyadh, Saudi Arabia.

With regard to the actual measurements, again we see that the recombination of a polyatomic molecule (TMA) has a recombination rate little different from that of other polyatomic ions. The attachment behavior on the other hand is completely different for TMA and DMA. This is the striking difference between recombination and attachment processes, where in the latter case, rate coefficients for molecules of the same families such as halocarbons can differ by as much as 5 orders of magnitude<sup>24</sup> while DR rates fall within a narrow range<sup>25</sup>. This may be because in DR, the process passes via a myriad of Rydberg states which take part in the electron capture process while for DEA, it must involve a direct transition from the neutral to the final ionic state, and the availability of such as state will determine the likelihood of the process.

## Notes

The authors declare no competing financial interest.

### ■ ACKNOWLEDGMENTS

S. Alshammari thanks the King Abdulaziz City for Science and Technology (KACST) for funding this work under grant no: 162-28 which underlies this manuscript. Valuable discussions with Dr. Bertrand Rowe are also gratefully acknowledged.

### ■ REFERENCES

- (1) S. L Sihto, et al., Atmospheric sulphuric acid and aerosol formation: implications from atmospheric measurements for nucleation and early growth mechanisms, *Atmos. Chem. Phys.*, 2006, v6, 4079-4091.
- (2) M. E. Erupe, A. A. Viggiano, S. H. Lee, The effect of trimethylamine on atmospheric nucleation involving H<sub>2</sub>SO<sub>4</sub>, *Atmos. Chem. Phys.*, 2011, v11, 4767-4775.
- (3) T. Kurtén, V. Loukonen, H. Vehkamäki, M. Kulmala, Amines are likely to enhance neutral and ion-induced sulfuric acid-water nucleation in the atmosphere more effectively than ammonia, *Atmos. Chem. Phys.*, 2008, v8, 4095-4103.
- (4) J. Almeida, S. Schobesberger, J. Kirkby, Molecular understanding of sulfuric acid-amine particle nucleation in the atmosphere, *Nature*, 2013, v502, 359-363.
- (5) A. P. Praplan, F. Bianchi, J. Dommen, U. Baltensperger, Dimethylamine and ammonia measurements with ion chromatography during the CLOUD4 campaign, *Atmos. Meas. Tech.*, 2012, v5, 2161-2167.
- (6) J. Kirkby, J. Curtius, J. Almeida, J. Duplissy, S. Ehrhart, A. Franchin, S. Gagne, L. Ickes, A. Kurten, A. Kupc, A. Metzger, F. Riccobono, L. Rondo, M. Kulmala, Role of sulphuric acid, ammonia and galactic cosmic rays in atmospheric aerosol nucleation, *Nature*, 2011, v476, 429-433.
- (7) D. C. McKean, The structure of dimethylamine, *J. Chem. Phys.*, 1983, v79, 2095.
- (8) L. Lehfaoui, C. Rebrion-Rowe, S. Laube, J. B. A. Mitchell, B. R. Rowe, The dissociative recombination of hydrocarbon ions: I. Light alkanes, *J. Chem. Phys.*, 1997, v106, 5406-5412.
- (9) Y. Ikezoe, S. Matsuoka, M. Takebe, A. Viggiano, *Ion-Molecule Reaction Rate Constants through 1986*, The Mass Spectroscopy Society of Japan, Tokyo, 1987.
- (10) R. Deloche, P. Monchicourt, M. Cheret, F. Lambert, High-pressure helium afterglow at room temperature, *Phys. Rev A*, 1976, v13, p 1140.

- (11) X. Urbain, *Dissociative Recombination, Theory, Experiment and Applications IV*, Eds; By M. Larson, J.B.A. Mitchell, I.F. Schneider, *World Scientific, Singapore*, 1999, p 131.
- (12) J. Glosik, G. Bano, R. Plasil, A. Luca, P. Zakouril, Study of the electron ion recombination in high pressure flowing afterglow: recombination of  $\text{NH}_4^+(\text{NH}_3)_2$ , *Int. J. Mass Spectr.*, 1999, v189 (2-3), 103-113.
- (13) C. Rebrion-Rowe, L. Lehfaoui, B. R. Rowe, J. B. A. Mitchell, The dissociative recombination of hydrocarbon ions: II Alkene and alkyne derived species, *J. Chem. Phys.* 1998, v108, 7185–7189.
- (14) P. F. Wilson, M. J. McEwan, M. Meot-Ner, Reactions of  $\text{CH}_3\text{OCH}_2^+$  with nitrogen bases: a mechanism for the formation of protonated imines, *Int. J. Mass Spectrom. Ion Proc.*, 1994, v132, 149–152.
- (15) M. S. B. Munson, Ionic Reactions in Gaseous Amines, *J. Phys. Chem.*, 1966, v70, 2034-2038.
- (16) J. A. Herman, K. Herman, T. B. McMahan, Ion-molecule reactions in methylamine and dimethylamine and trimethylamine systems, *Journal of the American Society for Mass Spectrometry*. 1991, v2, 220-225.
- (17) L. Hellner, L. W. Sieck, High-pressure photoionization mass spectrometry. Effect of internal energy and density on the ion-molecule reactions occurring in methyl, dimethyl, and trimethylamine *Int. J. Chem. Kin.*, 1973, V, 177-186.
- (18) R. D. Cates, M. T. Bowers, Energy transfer in ion-molecule association reactions. Dependence of collisional stabilization efficiency on the collision gas. *J. Am. Chem. Soc.*, 1980, v102, 3994-3996.
- (19) N. G. Adams, D. Smith, Measurements of the dissociative recombination coefficients for several polyatomic ion species at 300 K, *Chem. Phys. Lett.*, 1988, v144, 11–14.
- (20) J. A. Culbertson, E. P. Grimsrud, Fates of the molecular anions of  $\text{SF}_6$  and  $\text{C}_7\text{F}_{14}$  upon recombination with positive ions, *J. Mass Spectrom. & Ion Proc.*, 1995, v149/150, 87-98.
- (21) D. Smith, N.G. Adams E. , Alge, Attachment coefficients for the reactions of electrons with  $\text{CCl}_4$ ,  $\text{CCl}_3\text{F}$ ,  $\text{CCl}_2\text{F}_2$ ,  $\text{CHCl}_3$ ,  $\text{Cl}_2$  and  $\text{SF}_6$  determined between 200 and 600 K using the FALP technique, *J. Phys. B.*, 1984, v17, p 461.
- (22) S. Carles, J. L. Le Garrec, J. B. A. Mitchell, Electron and ion reactions with hexamethyldisiloxane and pentamethyldisiloxane, *J. Chem. Phys.*, 2007, v127, p 144308.
- (23) Allan N. Hayhurst, John M. Goodings, Stephen G. Taylor, The effects of applying electric fields on the mass spectrometric sampling of positive and negative ions from a flame at atmospheric pressure, *Combustion and Flame Journal*, 2014, v161, 3249-3262.
- (24) L. G. Christophorou, D. L. McCorkle, A. A. Christodoulides, *Electron-Molecule Interactions and Their Application*, Eds; By L. G. Christophorou, *Academic: Orlando*, 1984, VI. 1.
- (25) A. I. Florescu-Mitchell, J. B. A. Mitchell, Dissociative recombination, *Phys. Rep.*, 2006, v430, 277–374.